J|A|C|S ARTICLES

Published on Web 02/11/2010

Contact Geometry Symmetry Dependence of Field Effect Gating in Single-Molecule Transistors

Trilisa M. Perrine† and Barry D. Dunietz*

Department of Chemistry, University of Michigan, Ann Arbor, Michigan 48109

Received August 3, 2009; E-mail: bdunietz@umich.edu

Abstract: The geometric aspects for the functionality of a molecule-based field effect transistor (FET) are analyzed. A computational study is performed on molecular models involving a well-defined conjugation plane coupled to gold-based electrodes through thiol bonding. Transport gating of the FET is shown to depend on a symmetry-breaking effect induced by the gating field. This effect is also related to the orientation of the field relative to the gold−thiol bonds, the molecular conjugation plane, and the overall symmetry of the device. First, it is found that the presence of a center of inversion in the bulk-coupled molecular system results in the cancellation of the transisting response. Second, a mirror plane of the molecule−bulk system, which includes the transport vector, will cancel the gating response to fields oriented perpendicular to that mirror plane. The symmetry properties are determined for the bulk contacted molecular junction.

Molecular electronics have recently been in the center of increasing experimental and computational research efforts. This interest stems mainly from the prospect of fabricating highly efficient electronic devices utilizing the unique properties of single molecules.[1−37] A range of fabrication techniques have been employed to achieve molecule-based field effect transistors (FETs).[27,28,31,32,38] Theoretical studies have modeled the behavior due to a gating field at the molecular level as well.[39−46] In addition, the study of electron transmission through molecular systems using symmetry analysis of the transmission function

† Current address: Ohio Northern University, Ada, OH 45810.

(1) Reed, M. A.; Zhou, C.; Muller, C. J.; Burgin, T. P.; Tour, J. M. *Science* **1997**, *278*, 252–254.
(2) Stipe, B. C.; Rezaei, M. A.; Ho, W. *Science* **1998**, *280*, 1732–1735.
(3) Chen, J.; Reed, M. A.; Rawlett, A. M.; Tour, J. M. *Science* **1999**, *286*, 1550–1552.
(4) Collier, C. P.; Wong, E. W.; Belohradsky, M.; Raymo, F. M.; Stoddart, J. F.; Kuekes, P. J.; Williams, R. S.; Heath, J. R. *Science* **1999**, *285*, 391–394.
(5) Park, H.; Park, J.; Lim, A. K. L.; Anderson, E. H.; Alivisatos, A. P.; McEuen, P. L. *Nature* **2000**, *407*, 57–60.
(6) Collier, C. P.; Mattersteig, G.; Wong, E. W.; Luo, Y.; Beverly, K.; Sampaio, J.; Raymo, F. M.; Stoddart, J. F.; Heath, J. R. *Science* **2000**, *289*, 1172–1175.
(7) Rueckes, T.; Kim, K.; Joselevich, E.; Tseng, G. Y.; Cheung, C. L.; Lieber, C. M. *Science* **2000**, *289*, 94–97.
(8) Joachim, C.; Gimzewski, J. K.; Aviram, A. *Nature* **2000**, *408*, 541–548.
(9) Collins, P. G.; Arnold, M. S.; Avouris, P. *Science* **2001**, *292*, 706–709.
(10) Cui, X. D.; Primak, A.; Zarate, X.; Tomfohr, J.; Sankey, O. F.; Moore, A. L.; Moore, T. A.; Gust, D.; Harris, G.; Lindsay, S. M. *Science* **2001**, *294*, 571–574.
(11) Nitzan, A. *Annu. Rev. Phys. Chem.* **2001**, *52*, 681.
(12) Tour, J. M.; Rawlett, A. M.; Kozaki, M.; Yao, Y. X.; Jagessar, R. C.; Dirk, S. M.; Price, D. W.; Reed, M. A.; Zhou, C. W.; Chen, J.; Wang, W. Y.; Campbell, I. *Chem.—Eur. J.* **2001**, *7*, 5118–5134.
(13) Fan, F. R. F.; Yang, J. P.; Cai, L. T.; Price, D. W.; Dirk, S. M.; Kosynkin, D. V.; Yao, Y. X.; Rawlett, A. M.; Tour, J. M.; Bard, A. J. *J. Am. Chem. Soc.* **2002**, *124*, 5550–5560.
(14) Park, J.; Pasupathy, A. N.; Goldsmith, J. I.; Chang, C.; Yaish, Y.; Petta, J. R.; Rinkoski, M.; Sethna, J. P.; Abruna, H. D.; McEuen, P. L.; Ralph, D. C. *Nature* **2002**, *417*, 722–725.
(15) Liang, W. J.; Shores, M. P.; Bockrath, M.; Long, J. R.; Park, H. *Nature* **2002**, *417*, 725–729.
(16) Luo, Y.; Collier, C. P.; Jeppesen, J. O.; Nielsen, K. A.; Delonno, E.; Ho, G.; Perkins, J.; Tseng, H. R.; Yamamoto, T.; Stoddart, J. F.; Heath, J. R. *ChemPhysChem* **2002**, *3*, 519.
(17) Adams, D. M.; et al. *J. Phys. Chem. B* **2003**, *107*, 6668–6697.
(18) Metzger, R. M. *Chem. Rev.* **2003**, *103*, 3803–3834.
(19) Nazin, G. V.; Qiu, X. H.; Ho, W. *Science* **2003**, *302*, 77–81.
(20) Nitzan, A.; Ratner, M. A. *Science* **2003**, *300*, 1384–1389.
(21) Kushmerick, J.; Lazorcik, J.; Patterson, C.; Shashidhar, R.; Seferos, D.; Bazan, G. *Nano Lett.* **2004**, *4*, 639–642.
(22) Xiao, X.; Xu, B. Q.; Tao, N. *Nano Lett.* **2004**, *4*, 267–271.
(23) Xiao, X.; Xu, B. Q.; Tao, N. *Angew. Chem., Int. Ed.* **2004**, *45*, 6148–6152.
(24) Guisinger, N.; Greene, M.; Basu, R.; Baluch, A.; Hersam, M. *Nano Lett.* **2004**, *4*, 55–59.
(25) McCreery, R. L. *Chem. Mater.* **2004**, 4477–4496.
(26) Fan, F.-R.; Yao, Y.; Cai, L.; Cheng, L.; Tour, J.; Bard, A. *J. Am. Chem. Soc.* **2004**, *126*, 4035–4042.
(27) Piva, P. G.; DiLabio, G. A.; Pitters, J. L.; Zikovsky, J.; Rezeq, M.; Dogel, S.; Hofer, W. A.; Wolkow, R. A. *Nature* **2005**, *435*, 658–661.
(28) Xu, B. Q.; Xiao, X. Y.; Yang, X.; Zang, L.; Tao, N. J. *J. Am. Chem. Soc.* **2005**, *127*, 2386–2387.
(29) Chen, F.; He, J.; Nuckolls, C.; Roberts, T.; Klare, J. E.; Lindsay, S. *Nano Lett.* **2005**, *5*, 503–506.
(30) Kitagawa, K.; Morita, T.; Kimura, S. *J. Phys. Chem. B* **2005**, *109*, 13906–13911.
(31) Natelson, D.; Yu, L. H.; Ciszek, J. W.; Keane, Z. K. T. J. M. *Chem. Phys.* **2006**, *324*, 267–275.
(32) Keane, Z. K.; Ciszek, J. W.; Tour, J. M.; Natelson, D. *Nano Lett.* **2006**, *6*, 1518–1521.
(33) Zhirnov, V. V.; Cavin, R. K. *Nat. Mater.* **2006**, *5*, 11–12.
(34) Tang, J.; Wang, Y.; Nuckolls, C.; Wind, S. J. *J. Vac. Sci. Technol., B* **2006**, *24*, 3227–3229.
(35) Tang, J. Y.; Wang, Y. L.; Klare, J. E.; Tulevski, G. S.; Wind, S. J.; Nuckolls, C. *Angew. Chem., Int. Ed.* **2007**, *46*, 3892–3895.
(36) Venkataraman, L.; Park, Y. S.; Whalley, A. C.; Nuckolls, C.; Hybertsen, M. S.; Steigerwald, M. L. *Nano Lett.* **2007**, *7*, 502–506.
(37) Chen, F.; Hihath, J.; Huang, Z.; Li, X.; J., T. N. *Annu. Rev. Phys. Chem.* **2007**, *58*, 535–564.
(38) Hamadani, B. H.; Corley, D. A.; Ciszek, J. W.; Tour, J. M.; Natelson, D. *Nano Lett.* **2006**, *6*, 1303–1306.
(39) DiVentra, M.; Pantelides, S. T.; Lang, N. D. *Appl. Phys. Lett.* **2000**, *76*, 3448–3450.
(40) Bratkovsky, A. M.; Kornilovitch, P. E. *Phys. Rev. B* **2003**, *67*, 115307.
(41) Yang, Z.; Lang, N. D.; DiVentra, M. *Appl. Phys. Lett.* **2003**, *82*, 1938–1940.

 10.1021/ja906234v

has been shown to provide fundamental insight into the molecule-based transport.[47–49] However, due to the formidable practical challenges, it still remains to achieve a reproducible and robust scheme that can scale up the fabrication of single-molecule devices to an industrial scale. Here we concentrate on the functionality of molecular scale electronic devices as field effect transistors to illuminate the key structural requirments for enhancing gating behavior.

We study fundamental symmetry-based aspects that underlie the gating functionality by employing an idealized model to analyze the effect of a gating field. In this simplified picture the potential bias is dropped over the molecular system in a uniform fashion perpendicular to the transport vector. This is a reasonable approximation when considering gating devices which span a source drain distance that is longer than the length across which the gating field is generated. Although this is not the case for molecular scale devices, symmetry aspects explored here will still impact the functionality of devices where the electrode screening of the gating potential is important. We point to the study by Ghosh et al.[42] that provides for a fundamental approach to address gating potential contacts in addition to the source drain contacts. The transmission functions of each model system are computed under the same strength applied electric fields, which allow for direct comparison of the efficacy of the gating fields in shifting the transmission.

We previously reported by means of computational modeling a symmetry-breaking effect, which is crucial for gating functionality.[50] This effect is related to the contact geometries and the gating field orientations. The molecular model device is shown in Figure 1. This conjugated system resembles the widely studied device based on functionalized three phenyl ring molecules for which current-switching properties have been reported.[3] The molecule is bonded to the metal leads through thiol groups on both ends. We explored two geometric isomers of the conjugated molecule bonded to gold-based bulk material, in which the two gold−thiol bonds form a plane perpendicular to the conjugation plane. The two isomers differ in the relative position of the two gold−thiol bonds to the conjugation plane, leading to either a *cis* or *trans* arrangement relative to the transport vector, which lies in the conjugation plane. The gating was observed only for the *cis* isomer with fields oriented perpendicular to the current flow direction and the conjugation plane.[50] We have attributed this important structure−function relation of the FET to a fundamental symmetry-breaking effect on the electronic orbitals that is produced by the applied gating field.

Further understanding at the atomic level is still necessary to optimize the functionality of molecular scale FETs. We use as models thiol−metal contacted systems. In this study we provide the general symmetry relations that must be satisfied

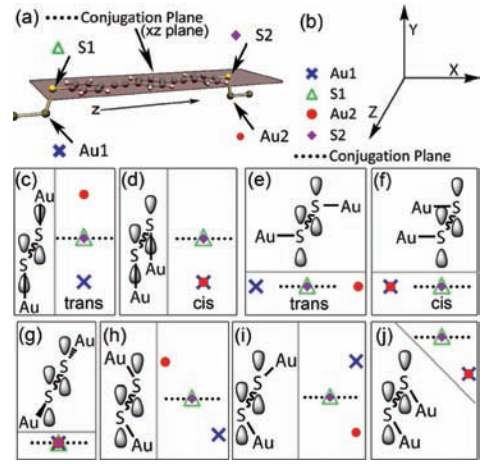

Figure 1. (a) Illustration of the general molecular configuration of the device region, where the electrodes are represented only by the single contacted thiolated gold atom. (b) Legend for the projected representations of the system and axis convention for the 3D representations. The molecular axis and gold wires are parallel to the *z* axis; the conjugation plane is parallel to the *xz* plane. The projected representations are projected onto the *xy* plane. (c−j) Contact geometries of considered model systems. Two representations are shown for each model. The first representation is a pseudo-three-dimensional (pseudo-3D) drawing of the system in which the sulfur and gold atoms of each contact are shown and the π system of the conjugated molecule is represented by p orbitals on the sulfur atoms. The second representation is a projection of the pertinent aspects of the device onto the *xy* plane.

by the configuration of the molecular bridge and the bulk material to achieve optimal response to a gating field, and more specifically those which will quench gating. The gating response is eliminated by the presence of either a center of inversion symmetry (*i*) or a mirror plane that includes the flux vector and which is perpendicular to the gating field orientation. This mirror plane is *parallel* to the current flow direction and is therefore here denoted as $\sigma_{\|}$, whereas mirror planes *perpendicular* to the transport vector are labeled as $\sigma_{\perp}$. Fabrication schemes, which satisfy the indicated symmetry conditions, are, therefore, indicated to yield enhanced functionality.

The geometries for the organic molecules are optimized at the DFT level using the B3LYP[51,52] functional and the LANL2DZ[53] basis set by employing QChem 3.1.[54] In the single gold atom wire models (see Figure 1) a single Au atom is bonded to the terminal thiols in the optimization. The bond lengths and angles of the optimized geometries are then kept fixed, while the dihedral angle is adjusted to generate the various orienations of the bulk model to the contacted molecule as illustrated in Figure 1. Additional models involve flat gold surfaces, where the geometries are obtained by connecting each end of the optimized organic portion of the system to a perfect Au(111) surface through the thiol at a perfect hollow site. Electronic integrals used for the electron transmission calculations are evaluated with several gating field strengths at the DFT level indicated above. For the transport properties, we follow the scattering-based picture of molecular conductance (Landauer formalism)[55−57] based on the Green function formalism as described in detail by others.[58–64]

(42) Ghosh, A. W.; Rakshit, T.; Datta, S. *Nano Lett.* **2004**, *4*, 565–568.
(43) Boudjella, A.; Zhongfang Jin, A.; Savaria, Y. *Jpn. J. Appl. Phys.* **2004**, *43*, 3831–3837.
(44) Choi, Y. C.; Kim, W. Y.; Park, K.-S.; Tarakeshwar, P.; Kim, K. S.; Kim, T.-S.; Lee, J. Y. *J. Chem. Phys.* **2005**, *122*, 094706.
(45) Son, Y.-W.; Ihm, J.; Cohen, M. L.; Louie, S. G.; Choi, H. J. *Phys. Rev. Lett.* **2005**, *95*, 216602.
(46) Ke, S. H.; Baranger, H. U.; Yang, W. *Phys. Rev. B* **2005**, *71*, 113401.
(47) Solomon, G. C.; Gagliardi, A.; Pecchia, A.; Frauenheim, T.; Carlo, A. D.; Reimers, J. R.; Hush, N. S. *J. Chem. Phys.* **2006**, *125*, 184702.
(48) Solomon, G.; Gagliardi, A.; Pecchia, A.; Frauenheim, T.; DiCarlo, A.; Reimers, J.; Hush, N. *Nano Lett.* **2006**, *6*, 2431–2437.
(49) Gagliardi, A.; Solomon, G. C.; Pecchia, A.; Frauenheim, T.; Carlo, A. D.; Hush, N. S.; Reimers, J. R. *Phys. Rev. B* **2007**, *75*, 174306.
(50) Perrine, T.; Dunietz, B. D. *Phys. Rev. B* **2007**, *75*, 195319.
(51) Becke, A. D. *J. Chem. Phys.* **1993**, *98*, 1372.
(52) Becke, A. D. *J. Chem. Phys.* **1993**, *98*, 5648.
(53) Wadt, W. R.; Hay, J. P. *J. Chem. Phys.* **1985**, *82*, 299.
(54) Shao, Y.; et al. *Phys. Chem. Chem. Phys.* **2006**, *8*, 3172–3191.
(55) Landauer, R. *Philos. Mag.* **1970**, *21*, 863.
(56) Bagwell, P. F.; Orlando, T. P. *Phys. Rev. B* **1989**, *40*, 1456–1464.
(57) Imry, Y.; Landauer, R. *Rev. Mod. Phys.* **1999**, *71*, S306–S312.

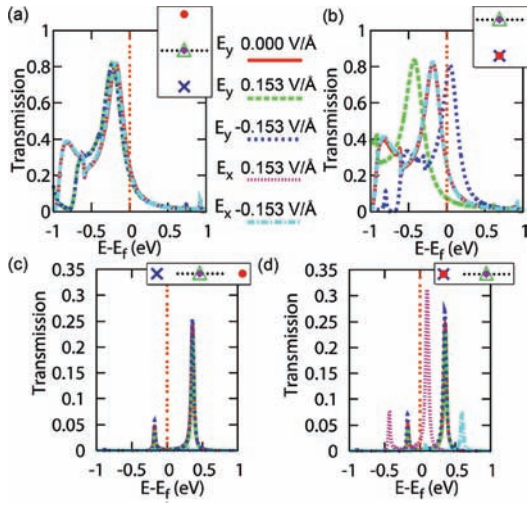

Figure 2. Transmission functions of four model systems illustrated in Figure 1c−f. The functions are drawn for no gating electric field, a ±0.153 V/Å electric field parallel to the *x* axis, and a ±0.153 V/Å electric field parallel to the *y* axis. The corresponding model systems are drawn for (a) in Figure 1c, for (b) in Figure 1d, for (c) in Figure 1e, and for (d) in Figure 1f.

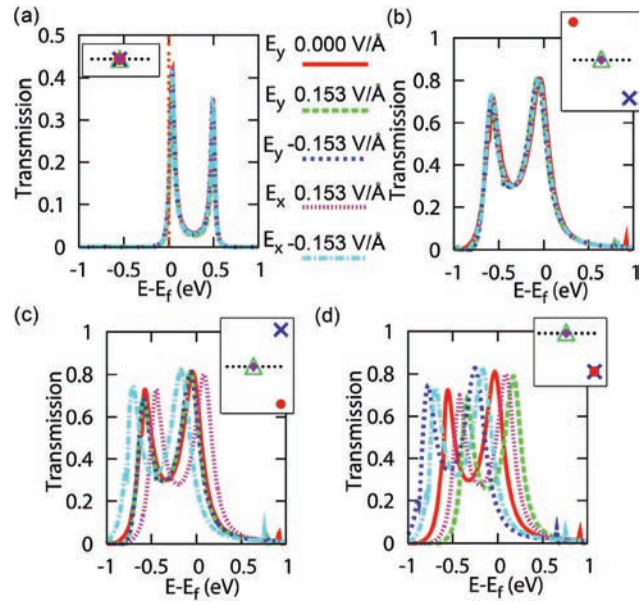

Figure 3. Transmission functions of model systems illustrated in Figure 1g−j. The functions are drawn for no gating electric field, a ±0.153 V/Å electric field parallel to the *x* axis, and a ±0.153 V/Å electric field parallel to the *y* axis. The corresponding model systems are drawn for (a) in Figure 1g, for (b) in Figure 1h, for (c) in Figure 1i, and for (d) in Figure 1j.

The previously studied *cis* and *trans* contact geometries are illustrated in Figure 1c,d. As a result of the symmetry aspects summarized above,[50] the transmission through the *trans* conformer does not change by application of an electric field directed parallel to either the *x* or *y* axis (see Figure 1 for a definition of these axes). The *cis* isomer, on the other hand, features a gating response only for a field oriented perpendicular to the conjugation plane (along the *y* axis). The electronic transmission of these *trans* and *cis* configurations is plotted in parts a and b, respectively, of Figure 2. To generalize the previously reported symmetry requirements for a gating response, we consider a more elaborate set of geometric aspects of the molecular FET model with a well-defined conjugation plane. Additional considered configurations involving single gold atom wires are represented in Figure 1e−g. In (e) and (f) the thiol bonds lie within the conjugation plane to form another pair of *cis* and *trans* configurations, whereas in (g) the two bonds are placed along the line defined by the two sulfur atoms.

Briefly, we find that for the *cis*/*trans* pairs of configurations, which are illustrated in parts c and d and parts e and f of Figure 1, the gating response is noted only for one gating field orientation for each *cis* configuration, and no response is observed in the *trans* isomers (Figure 2). The effective gating direction is determined by the relationships of the symmetry of the system, the field orientation, and the thiol bonding configuration. As discussed above, a gating field oriented *perpendicular* to the conjugation plane gates the *cis* configuration of the isomer illustrated in Figure 1d. However, it is only the field oriented *parallel* to the conjugation plane that gates the *cis* isomer, illustrated in Figure 1f. In this *cis* isomer (Figure 1) the conjugation plane is coincident with the plane formed by the gold−thiol bonds. To complete these observations, the transmission through a model system in which all of the gold atoms lie along the molecular axis (*z* axis) which contains the two sulfurs (see Figure 1g) is considered. It is found that the transmission as shown in Figure 3a for this higher symmetry configuration is unaffected by an electric field parallel to either the *x* axis or *y* axis. This is similar to the considered *trans* isomers, where the application of any gating field is unable to cause a symmetry-breaking effect.

To summarize the conditions for the gating response for the above wire models, we find that if the contact gold atoms are *trans* to each other (or along the molecular axis itself), then any gating field perpendicular to the transport direction will fail to shift the transmission of the molecular device. Each of these *trans* models contains a center of inversion in the contacted molecule−bulk system, which negates the gating effect. In the cases of reduced symmetry where the contact gold atoms form a *cis* relation with respect to the conjugation plane, an applied field in the corresponding direction (i.e., in the plane formed by the gold−thiol bonds) will gate the transmission. Therefore, the *cis* and *trans* orientations of the contact gold atoms in the wire models and the relative orientation of the electric field define the direction of a functional gating field for a molecular FET.

To continue and further generalize the identified conditions for a gating response in molecular FETs, we consider additional interaction schemes between the organic molecule and the electrode. In each of the above model systems, the gold−thiol bonds are either parallel or perpendicular to both the conjugation plane and the applied electric field. For complete analysis of the molecular FET structure function relations, additional configurational aspects involving the conjugation plane and the thiol−gold bonds need to be considered.

(58) Samanta, M. P.; Tian, W.; Datta, S.; Henderson, J. I.; Kubiak, C. P. *Phys. Rev. B* **1996**, *53*, R7626–R7629.
(59) Tian, W.; Datta, S.; Hong, S.; Reifenberger, R.; Henderson, J. I.; Kubiak, C. P. *J. Chem. Phys.* **1998**, *109*, 2874–2882.
(60) Mujica, V.; Nitzan, A.; Mao, Y.; Davis, W.; Kemp, M.; Roitberg, A.; Ratner, M. A. *Adv. Phys. Chem.* **1999**, *107*, 403.
(61) Yaliraki, S. N.; Roitberg, A. E.; Gonzalez, C.; Mujica, V.; Ratner, M. A. *J. Chem. Phys.* **1999**, *111*, 6997–7002.
(62) Xue, Y.; Datta, S.; Ratner, M. A. *J. Chem. Phys.* **2001**, *115*, 4292–4299.
(63) Baer, R.; Neuhauser, D. *J. Am. Chem. Soc.* **2002**, *124*, 4200–4201.
(64) Liu, C.; Walter, D.; Neuhauser, D.; Baer, R. *J. Am. Chem. Soc.* **2003**, *125*, 13936–13937.

We next extend the wire models to explore the effect of the relative orientation of the conjugation plane and the electrode models. We examine three wire model systems with the gold−thiol bonds at an angle of 60° with respect to the conjugation plane. These three models are shown in Figure 1h−j. The model in Figure 1h has gold atoms which are *trans* to each other in both the *x* and *y* directions. Similarly, the model shown in Figure 1j has gold atoms which are *cis* to each other in both the *x* and *y* directions. Though these models are of lower symmetry than those discussed above, it is found that they respond to the application of an electric field similarly to the higher symmetry *cis* and *trans* systems. The transmission of the fully *trans* model (Figure 1h), which contains a center of inversion, shows no response to a field either parallel or perpendicular to the conjugation plane (Figure 3b). The transmission through the fully *cis* model (Figure 1j) shifts through the application of either orientation of an electric field (see Figure 3d). These observations confirm the criteria stated above. The model system in which the gold atoms are *cis* to each other along the *x* direction but *trans* to each other along the *y* direction (Figure 1i) contains no center of inversion. This model responds only to the electric field oriented parallel to the *x* axis (Figure 3c), which is the direction in which the gold wires are *cis* to each other.

These geometry relations are also reflected quantitatively in the strength of the gating response. For example, under the influence of a 0.153 V/Å gating field the transmission function of the model in Figure 1c is shifted only by 0.05 eV, while that of Figure 1i is shifted by 0.12 eV and that of Figure 1d is shifted by 0.25 eV. The corresponding drop in current due to the same gating field for the models in parts c and d of Figure 1 under a potential bias of 0.50 V are 10.8% and 70.3%, respectively.

We next explore surface bulk models. The interactions of a molecule with a surface are more complicated, in general, than can be fully identified by labels as simple as *cis* and *trans*, and we therefore must rely on more sophisticated symmetry analysis. To determine the transisting response upon bonding to surfaces, four additional systems were examined in which the wire models are replaced by perfect Au(111) plane models. These are drawn in Figure 4 using the same projection scheme as in Figure 1. The gold surfaces (electrode models) contacting the two sides of the molecular system are parallel in each case. In two of the models these surfaces are mirror images of each other and are, therefore, associated with *cis* isomers. For the other two models the surfaces are rotated 180° relative to each other; this results in a *trans*-like arrangement as illustrated in the figure. For both these *trans* and *cis* surface configurations there are two isomers where each differs by a 90° rotation of the conjugation plane about the current flow axis.

The corresponding computed transmission functions under various gating fields for the surface models are plotted in Figure 5. As with the simpler gold wire model systems, for both *trans* surface models the transmission is not shifted under the influence of any gating field oriented in the *xy* plane (perpendicular to the current flow axis). It is again only for the *cis* models that an orientation of the gating field which shifts the transmission can be identified.

For the *cis* surface models each surface atom has a corresponding atom on the opposite side; i.e., a mirror plane (*xy*) exists between and parallel to the surfaces and *perpendicular* to the transport vector ($\sigma_\perp$). In both *cis* models, there is also a mirror plane *parallel* to the transport vector ($\sigma_\parallel$) and the *yz* plane. A $\sigma_\parallel$ mirror plane is present for the *cis* arrangements of both of the considered bulk models (atomic wires and perfect Au(111) systems). This $\sigma_\parallel$ mirror plane (*yz*) eliminates the gating response for both models when the electric field is aligned parallel to the *x* axis (perpendicular to the $\sigma_\parallel$ mirror plane).

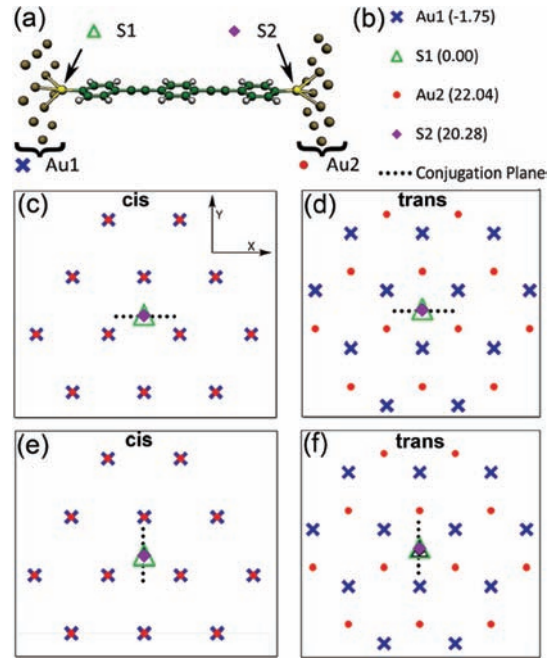

Figure 4. (a) Illustration of the general molecular configuration of the device region, where the electrodes are represented by a perfect (111) plane of gold atoms. (b) Legend for the atoms designated in the projected representations of the system (the *z* coordinate value of the gold−thiol atoms is noted in parentheses). The same designation of the axis as in Figure 1 is employed in these models. (c−f) Contact geometries of the models are represented on the *xy* plane. (c−e) Contact geometries of the considered model systems, where a projection of the pertinent aspects of the device onto the *xy* plane is provided.

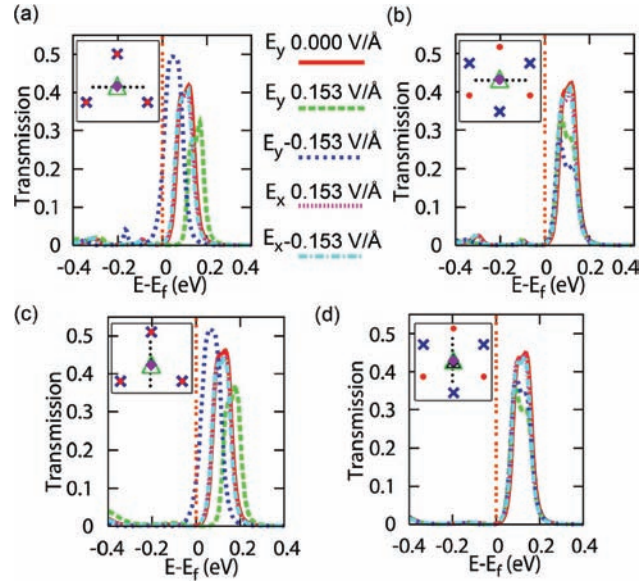

Figure 5. Transmission functions of model systems where the electrodes are contacted to the molecule through a perfect Au(111) plane illustrated in Figure 4c−f. The functions are drawn for no gating electric field, a ±0.153 V/Å electric field parallel to the *x* axis, and a ±0.153 V/Å electric field parallel to the *y* axis. The corresponding model systems are drawn for (a) in Figure 4c, for (b) in Figure 4d, for (c) in Figure 4e, and for (d) in Figure 4f.

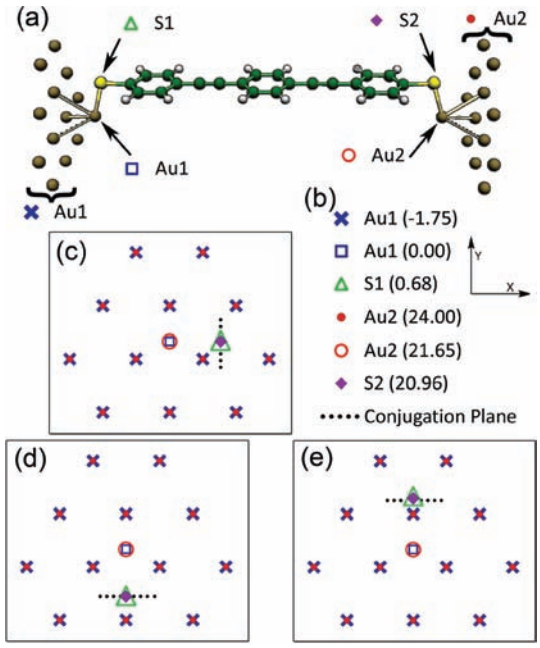

Figure 6. (a) Illustration of the general molecular configuration of the device region, where the electrodes are represented by a an adatom on a Au(111) plane. The adatom is used to contact the molecular thiolated system. (b) Legend for the atoms designated in the projected representations of the system. The same designation of the axis as in Figure 1 is employed in these models. The projected representations are projected onto the *xy* plane. (c−e) Contact geometries of the considered model systems, where a projection of the pertinent aspects of the device onto the *xy* plane is provided.

Finally, we consider models that extend the contact geometries by including thiol bonding to surface gold adatoms. Model systems of this type, which are more representative of experimental surface structures, are shown in Figure 6. In these models a single adatom is added to each of the parallel Au(111) surfaces at a perfect hollow site, and the molecular portion of the device is bonded to this adatom at the optimized bond length and angle of the model in Figure 1d. Three related models are shown in Figure 6 and are all *cis*-like in character; namely, there is no center of inversion for these models, and a $\sigma_\perp$ mirror plane lies between and parallel to the gold surfaces (perpendicular to the flux vector). The configurations shown in Figure 6d,e differ in the specific contact geometry, but have the same $\sigma_\parallel$ plane of symmetry (*yz* plane). In both of these models, as in many of the models discussed above, the transmission function is shifted only under the influence of an electric field directed along this $\sigma_\parallel$ plane and therefore parallel to the *y* axis. An electric field directed parallel to the *x* axis for these models and perpendicular to the $\sigma_\parallel$ plane has no effect on the transmission. The model drawn in Figure 6c has no $\sigma_\parallel$ plane of symmetry, as well as no center of inversion, though it does still contain the $\sigma_\perp$ plane. An electric field directed at any angle in the *xy* plane affects the transmission function; however, this response is not a clean shifting of the transmission function, as it is in the systems containing a $\sigma_\parallel$ plane of symmetry.

The presence of a center of inversion leads to a symmetry where the gating response is eliminated for any field oriented perpendicular to the flux vector. All models with a center of inversion do not respond to the applied field with a shift of the transmission function (see Figures 2a,c, 3a,b, and 5b,d). While all purely *trans* configurations contain a center of inversion, the *cis* configurations do not. The models which display gating behavior do not contain a center of inversion, but many of them are still highly symmetric. In both the wire and surface models, a gating response is obtained only for an electric field oriented so that it is not perpendicular to any $\sigma_\parallel$ mirror plane in the system (Figures 2b,d and 5a,c).

To conclude, there are two symmetry criteria that determine the gating response to a field aligned perpendicular to the flow axis. First, the presence of a center of inversion will cancel the gating response to the field. Second, the gating response will be eliminated if the applied field is perpendicular to a $\sigma_\parallel$ mirror plane of symmetry of the molecule−bulk system which lies parallel to the transport vector. Finally, a uniform and robust shifting of the transmission function of the system occurs when an applied electric field lies in a $\sigma_\parallel$ plane of symmetry of the contacted system. It is found that models that satisfy the symmetry criteria for gating activity and for enhanced response are indeed associated with a larger shift in the transmission function and therefore a larger gating effect.

Acknowledgment. B.D.D. acknowledges the University of Michigan and donors of the Petroleum Research Fund, administered by the American Chemical Society (through Grant 47118-G6), for financial support. We also acknowledge the National Energy Research Scientific Computing Center (NERSC) for awarding computing time.

Supporting Information Available: Complete list of authors for ref 54. This material is available free of charge via the Internet at http://pubs.acs.org.

JA906234V